pISSN 1229-845X, eISSN 1976-555X
J. Vet. Sci. (2014), **15**(2), 289-295
http://dx.doi.org/10.4142/jvs.2014.15.2.289
Received: 7 Jun. 2013, Revised: 25 Nov. 2013, Accepted: 21 Feb. 2014

JOURNAL OF
Veterinary Science

Original Article

Comparable bone healing capacity of different bone graft matrices in a rabbit segmental defect model

Jong Min Kim[1], Myoung Hwan Kim[2], Seong Soo Kang[3], Gonhyung Kim[2], Seok Hwa Choi[2,*]

[1]*Xenotransplantation Research Center, Biomedical Research Institute, Seoul National University Hospital, Seoul 153-832, Korea*
[2]*Veterinary Medical Center, Chungbuk National University, Cheongju 361-763, Korea*
[3]*College of Veterinary Medicine, Chonnam National University, Gwangju 500-757, Korea*

We compared the bone healing capacity of three different demineralized bone matrix (DBM) products applied using different carrier molecules (hyaluronic acid [HA] *vs.* carboxymethylcellulose [CMC]) or bone compositions (cortical bone *vs.* cortical bone and cancellous bone) in a rabbit segmental defect model. Overall, 15-mm segmental defects in the left and right radiuses were created in 36 New Zealand White rabbits and filled with HA-based demineralized cortical bone matrix (DBX), CMC-based demineralized cortical bone matrix (DB) or CMC-based demineralized cortical bone with cancellous bone (NDDB), and the wound area was evaluated at 4, 8, and 12 weeks post-implantation. DBX showed significantly lower radiopacity, bone volume fraction, and bone mineral density than DB and NDDB before implantation. However, bone healing score, bone volume fraction, bone mineral density, and residual bone area at 4, 8, and 12 weeks post-implantation revealed no significant differences in bone healing capacity. Overall, three DBM products with different carrier molecules or bone compositions showed similar bone healing capacity.

Keywords: bone graft substitutes, bone regeneration, carboxymethylcellulose, hyaluronic acid, rabbit

Introduction

Orthopedic surgery using autogenous bone graft is currently the standard method of treating bone defects. However, this therapy is subject to potential complications and morbidity associated with harvesting autogenous bones from the donor [25]. As a result, bone graft substitutes are widely used to enhance bone regeneration. Among such bone substitutes, demineralized bone matrix (DBM) is an allograft that is obtained from processes comprised of washing, demineralization with organic solvents, drying, and sterilization of cadaveric bones. Several reports demonstrated that DBM had osteo-inductive factors such as bone morphogenetic proteins (BMPs), induced adjacent cells into osteo-progenitor cells and promoted bone healing and osteo-conduction [4,7,9]. However, powdered or particulate forms of DBM have some limitations in clinical use, such as difficulty handling, tendency to migrate away from graft sites, and a lack of stability after surgery [10,12]. Many carrier materials from either natural or synthetic resources including glycerol, hyaluronic acid, lecithin, and polyorthoester have been developed to enhance the handling of DBM powder [8,17,19].

To date, various commercially available DBM products have been developed and evaluated in animal models with respect to bone healing capacity [13,14,24]. Such products have also been tested in other animal models such as those of spinal fusion [13,16,24] and small bone defects [4,7,15]. However, comparative studies using different types of DBM products have not been reported in an accurate fashion with regards to bone healing capacity and various bone parameters measured by different analytical methods. Therefore, in this study, we compared the bone healing effects of three different DBM products, hyaluronic acid (HA)-based demineralized cortical bone matrix (DBX), carboxylmethylcellulose (CMC)-based demineralized cortical bone matrix (DB), and CMC-based demineralized cortical bone matrix with cancellous bone (NDDB) using X-ray, micro-CT and histological methods in a rabbit segmental defect model.

*Corresponding author: Tel: +82-43-261-3144, Fax: +82-43-267-2595, E-mail: shchoi@cbnu.ac.kr

Table 1. The specification of three bone graft substitutes used in this study

	Composition ratio (W/W%)			Particle size (μm)
	Non-demineralized cancellous bone	Demineralized cortical bone	Carrier	
DBX	−	31	69 (4% HA)	212～850
DB	−	30	70 (3% CMC)	125～850
NDDB	12	18	70 (3% CMC)	125～850

DBX, hyaluronic acid (HA)-based demineralized cortical bone matrix; DB, carboxylmethylcelluose (CMC)-based demineralized cortical bone matrix; NDDB, CMC-based demineralized cortical bone matrix with cancellous bone.

Materials and Methods

Overview

Thirty eight, eight week old New Zealand White rabbits (2.2 kg ± 0.2) were used to evaluate *in vivo* bone healing effects of DBX, DB, and NDDB. Two rabbits were not subjected to treatment as a control and were only used for radiographic examination during the 12 weeks post-operation. DB and NDDB were kindly provided by Hans Biomed (Korea), while DBX putty (Synthes, USA) was purchased from the Musculoskeletal Transplant Foundation, Pennsylvania, USA. The specifications of the three bone graft substitutes are given in Table 1. Four rabbits from each group (total 12 rabbits per group) were sacrificed at 4, 8, or 12 weeks post-implantation. Fifteen mm segmental defects in the left and right radiuses were created in 36 New Zealand White rabbits and filled with DBX, DB or NDDB, and the wound area was evaluated at 4, 8, and 12 weeks post-implantation. This study was approved by the Institutional Animal Care and Use Committee of Chungbuk National University, Korea.

Surgical technique

Zoletil (15 mg/kg) and xylazine (5 mg/kg) were injected intramuscularly for anesthesia, after which the skin was incised to separate the subcutaneous tissue and expose the radius. Each 15-mm segmental defect was created in both the left and right radiuses in 38 New Zealand White rabbits, after which the defect was filled with either DBX, DB or NDDB. The defect was left empty in two rabbits as a control. Three bone graft substitutes were implanted into the radial defects in random order. An antibiotic (cefazolin 20 mg/kg) and an analgesic (tramadol 3 mg/kg) were then injected intramuscularly for three days.

Autopsy, radiographic and micro-computed tomographic (CT) evaluation

Four rabbits from each group were euthanized at 4, 8, or 12 weeks after surgical procedures, after which X-ray images were taken with an X-ray machine (Rotanode; Toshiba, Japan) from a distance of 100 cm (60 kVp and 300 mA) with an exposure time of 0.03 sec. Digital images were used to evaluate the degree of bone healing on the basis of the criteria described by Cook *et al.* [6]. The specific scores were as follows: no visible new bone formation, 0; minimal new disorganized bone, 1; disorganized new bone bridging grafted to host at both ends, 2; organized new bone of cortical density bridging at both ends, 3; loss of graft-host distinction, 4; and significant new bone and graft remodeling, 5. After X-ray images were taken, the radiuses were collected and fixed in 10% neutral buffered formalin. Three bone graft substitutes and samples taken at 4, 8, and 12 weeks after implantation were imaged using a micro-CT (Skyscan Desktop Micro-CT 1172; Skyscan, Belgium). The scanned data were reconstructed using software (NRecon; Skyscan). Bone mineral density (BMD) and the ratio of bone volume to total volume (BV/TV) of the three DBM products were calculated according to the program set by the software. Grey thresholds were set from 65 to 255 using image analysis software (CT-analyzer; Skyscan).

Histopathological evaluation

The samples were decalcified using a Shandon TBD-2 DECALCIFIER (Thermo Scientific, USA) and embedded in paraffin. The five tissue sections (100 m away from each section) obtained in 4-μm thickness were stained with hematoxylin and eosin. The samples were thoroughly observed under a microscope, and the regions involving proximal and distal host bone in the slides were photographed. Residual graft areas (mm^2) were then calculated using a digital image analyzer (Image Partner Software; Saram soft, Korea) to evaluate the rate of resorption of the grafts.

Statistical Analysis

The results are expressed as the mean ± standard deviation (SD). Levene's test for equality of variances was performed. If the variances were homogenic, one-way analysis of variance (ANOVA) was performed, followed by Dunnett's *t* test to identify significant differences among groups, if necessary.

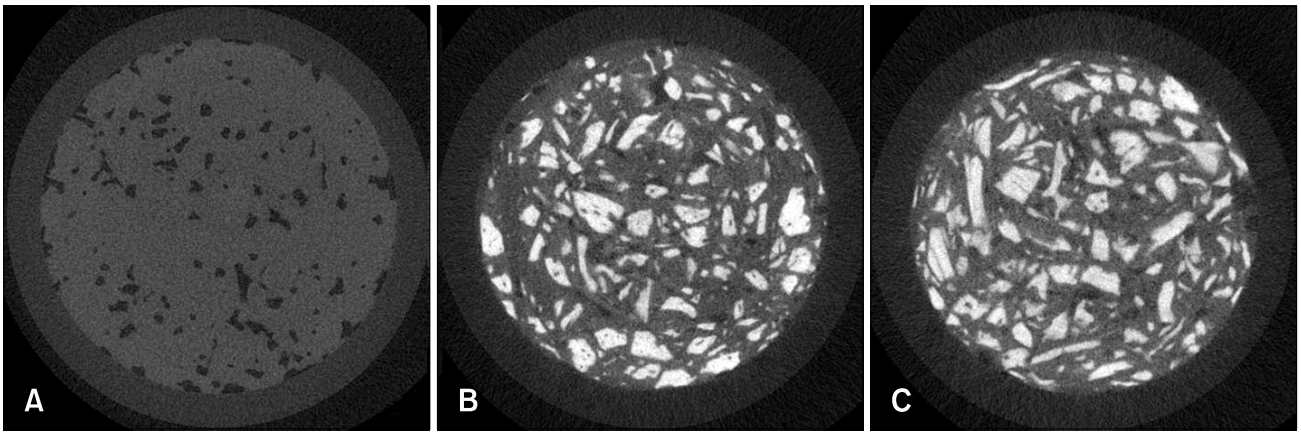

Fig. 1. Micro-CT images of DBX (A), DB (B), and NDDB (C). Three bone graft substitutes were imaged using a micro-CT. DBX clearly shows lower radiopacity than DB and NDDB, while there are few radiopaque particles in DBX.

Results

Physical characteristics of DBM products

Because the investigated DBM products have different compositions and carrier materials, we first examined their physical characteristics by micro-CT analysis. As shown in Fig. 1, the radiopacity of DB and NDDB was higher than that of DBX. Accordingly, many radiopaque particles of variable sizes were observed in both DB and NDDB, whereas there were no such particles in DBX on the three dimensional images (Fig. 1). Consistent with this finding, the bone mineral density (BMD) of DBX calculated by the image analysis program was significantly lower than those of DB and NDDB (0.20 ± 0.03 in DBX *vs.* 0.69 ± 0.04 and 0.65 ± 0.02 g/cm^3 in DB and NDDB, respectively $p < 0.01$). The ratio of bone volume to tissue volume (BV/TV; %) was also significantly lower in DBX than those of DB and NDDB (Table 2). Overall, DBX has a significantly lower calcium content, which is reflected by lower radiopacity, BMD, and BV/TV (%), than DB and NDDB, although DBX and DB have similar particle sizes (125 ~ 850 μm) and cortical bone content (~ 70%), suggesting that DBX is more thoroughly demineralized during the manufacturing process than the other two products.

Bone healing effects of DBM products by radiographic analysis

Following induction of 15-mm segmental bone defects in both the left and right radiuses, different DBM products were implanted and X-ray images were taken at 0, 4, 8, and 12 weeks. Callus formation, but no union, was observed in the untreated rabbits at 12 weeks after the surgery. DBX was similar to the no treatment group at 0 week post-implantation due to its low radiopacity. There were increased new bone densities, but no difference in DBX, DB, and NDDB at 4, 8, and 12 weeks post-implantation (Fig. 2). As shown in Fig. 3, bone healing scores measured by radiographic analysis increased from 0 to 1.28, 2.28, and 4.16 in the DBX group at 0, 4, 8, and 12 weeks post-implantation, respectively, and this trend did not differ significantly among groups.

Table 2. Bone parameters of three bone substitutes measured by image analysis

	BMD (g/cm^3)	BV/TV (%)
DBX	0.20 ± 0.03	1.23 ± 0.02
DB	0.69 ± 0.04*	90.37 ± 5.34*
NDDB	0.65 ± 0.02*	87.69 ± 6.52*

BMD: bone mineral density, BV: bone volume, TV: tissue volume, BV/TV (%): bone volume fraction. The values are the means ± standard deviation (SD) (n = 8). *$p < 0.01$ *vs.* DBX.

Micro-CT findings

BMD and bone volume fraction (%) of DBX were significantly lower than those of DB and NDDB before implantation (Table 2); however, they were surprisingly similar at 4 weeks post-implantation. Bone volume fraction decreased mildly between 8 and 12 weeks, but there were no statistical differences in bone volume fraction at 4, 8, and 12 weeks post-implantation among groups (Fig. 4).

The BMD of DBX increased from 0.2 to 0.32 g/cm^3, while those of DB and NDDB decreased from 0.69 and 0.65 to 0.28 and 0.47 g/cm^3 at 4 weeks post-implantation, respectively. However, the BMDs of the three groups at 8 weeks post-implantation were similar to those at 4 weeks post-implantation. BMD dramatically increased between 8 and 12 weeks post-implantation, but this trend did not differ among groups (Fig. 5).

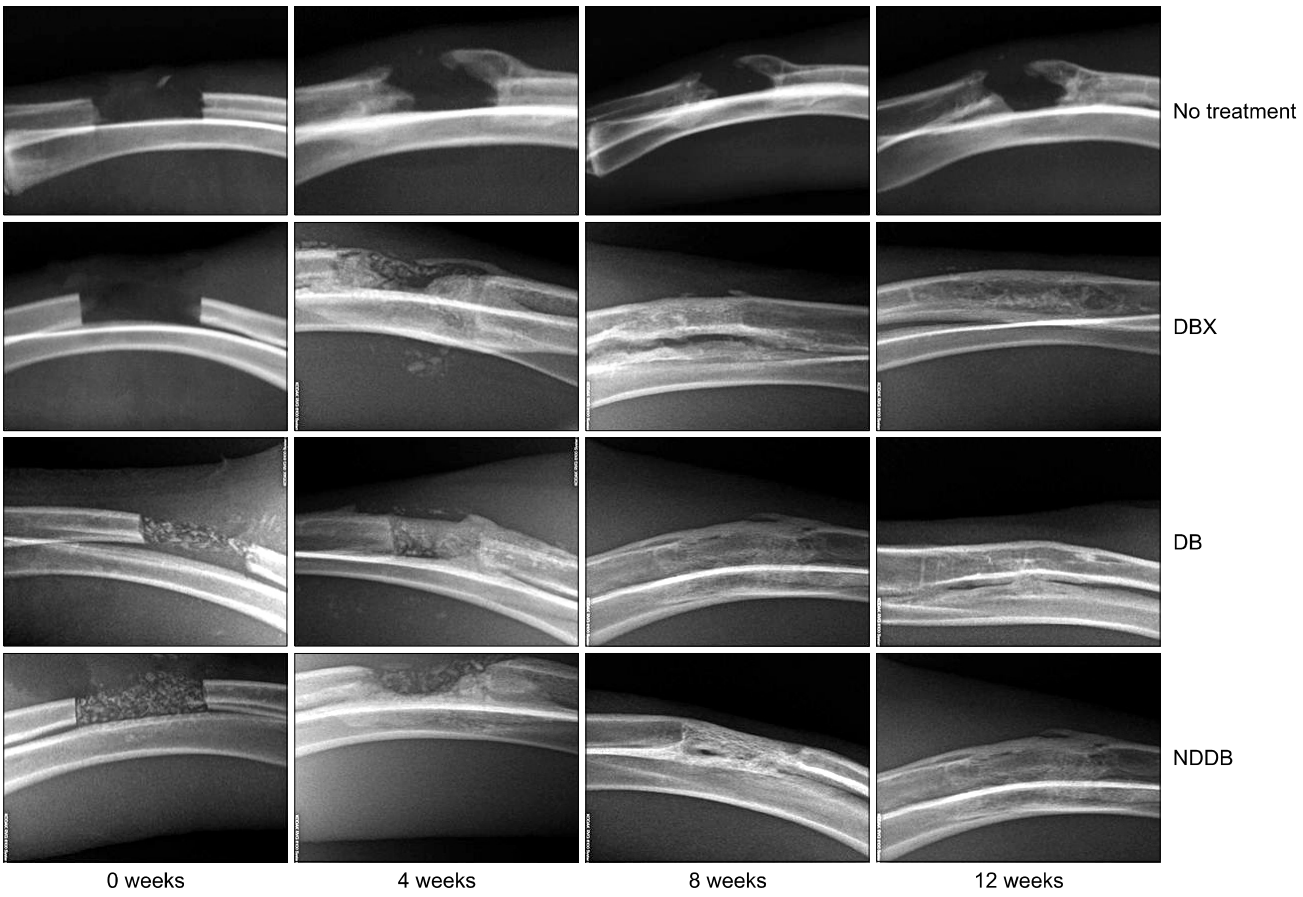

Fig. 2. Radiographic images of no treatment, DBX, DB, and NDDB at 0, 4, 8, and 12 weeks post-implantation. There was callus formation but no union in the no treatment group at 12 weeks after the surgery. DBX was similar to the no treatment at 0 weeks post-implantation due to its low radiopacity. There were increased new bone densities, but no difference in DBX, DB, and NDDB at 4, 8, and 12 weeks post-implantation.

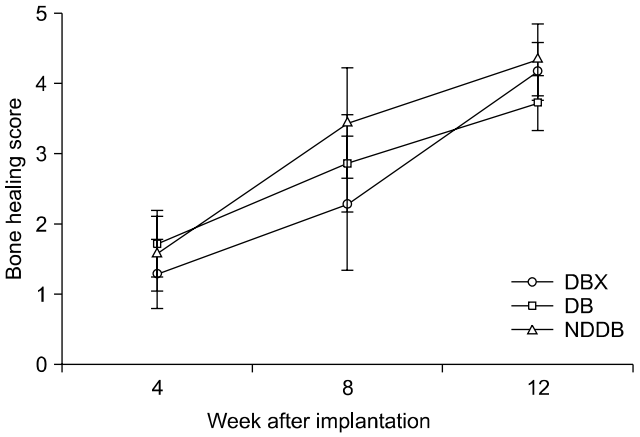

Fig. 3. Bone healing scores measured by radiographic image analysis. Four rabbits from each group were euthanized at 4, 8, or 12 weeks after surgical procedures, respectively, and X-ray images were taken with an X-ray machine. Digital images were used to evaluate the degree of bone healing based on the criteria defined by Cook *et al.* [6]. Bone healing scores increased nearly linearly during the experimental period, and there were no significant differences in this trend among groups. The values shown are the mean ± SD (n = 8).

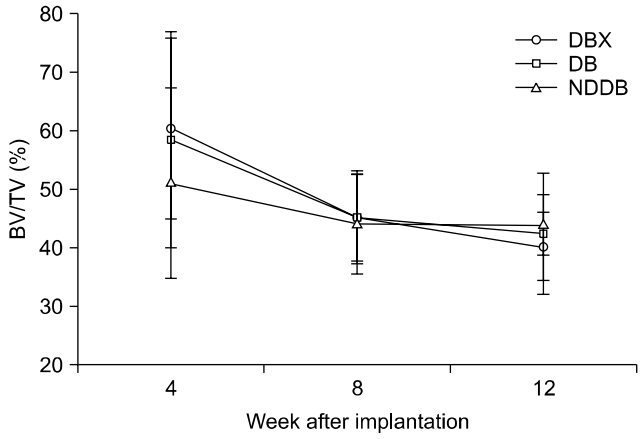

Fig. 4. Changes in bone volume fraction (%) after implantation. The samples from the euthanized rabbits were imaged using a micro-CT at 4, 8, and 12 weeks after implantation. The scanned data were reconstructed using software. Bone mineral density (BMD) and the ratio of bone volume to total volume (BV/TV) of three DBM products were calculated according to the program set by the software. The values are the mean ± SD (n = 8).

Histopathological findings

Histological examination showed that there were numerous new bone matrices and grafted DBM over all areas of the defect sites, and that the DBM particles were surrounded by newly formed bone matrix in all three groups at 4 weeks post-implantation. At 8 weeks post-implantation, all groups had less new bone tissue than at 4 weeks post-implantation, and initial signs of bone marrow formation evidenced by a meshwork of bone trabeculae inside bones were frequently observed. At 12 weeks post-implantation, bone remodeling processes appeared to be complete, and intact bone structures were easily observed in all three groups (Fig. 6).

Residual areas of the grafted DBM calculated from the

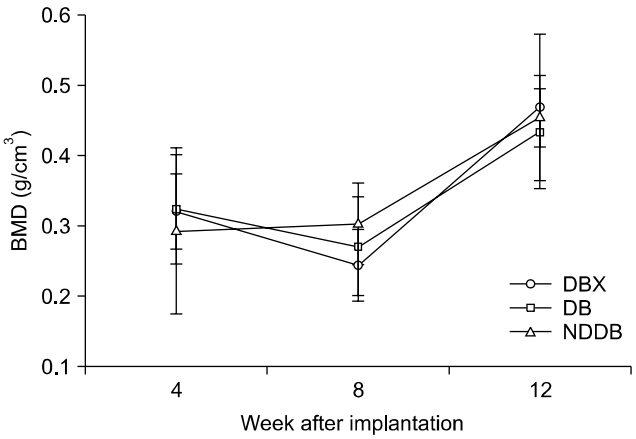

Fig. 5. Changes in bone mineral density after implantation. The samples from the euthanized rabbits were imaged using a micro-CT at 4, 8, and 12 weeks after implantation. The scanned data were reconstructed using the software. The BMD of the three DBM products were calculated according to program set by the software (CT-analyzer; Skyscan). The values are the mean ± SD (n = 8).

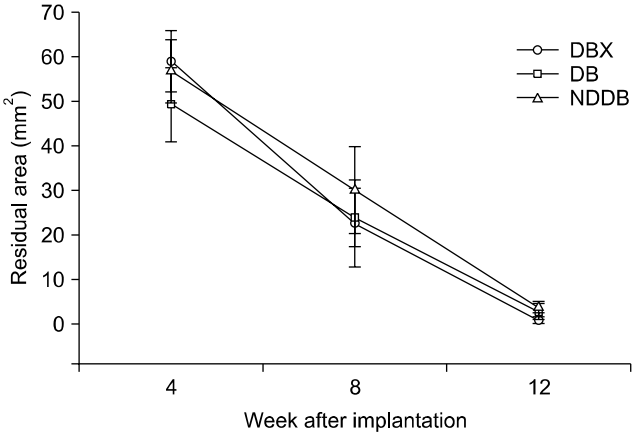

Fig. 7. Measurement of the residual area (mm^2) of DBX, DB, and NDDB after implantation. The samples were decalcified and embedded in paraffin. The five tissue sections (100 μm away from each section) were 4-μm thick and stained with H&E, after which they were thoroughly observed under a microscope and the regions of proximal and distal host bone in the slides were photographed. Residual graft areas (mm^2) were calculated using a digital image analyzer to evaluate the resorption rate of the grafts. The values are the mean ± SD (n = 8).

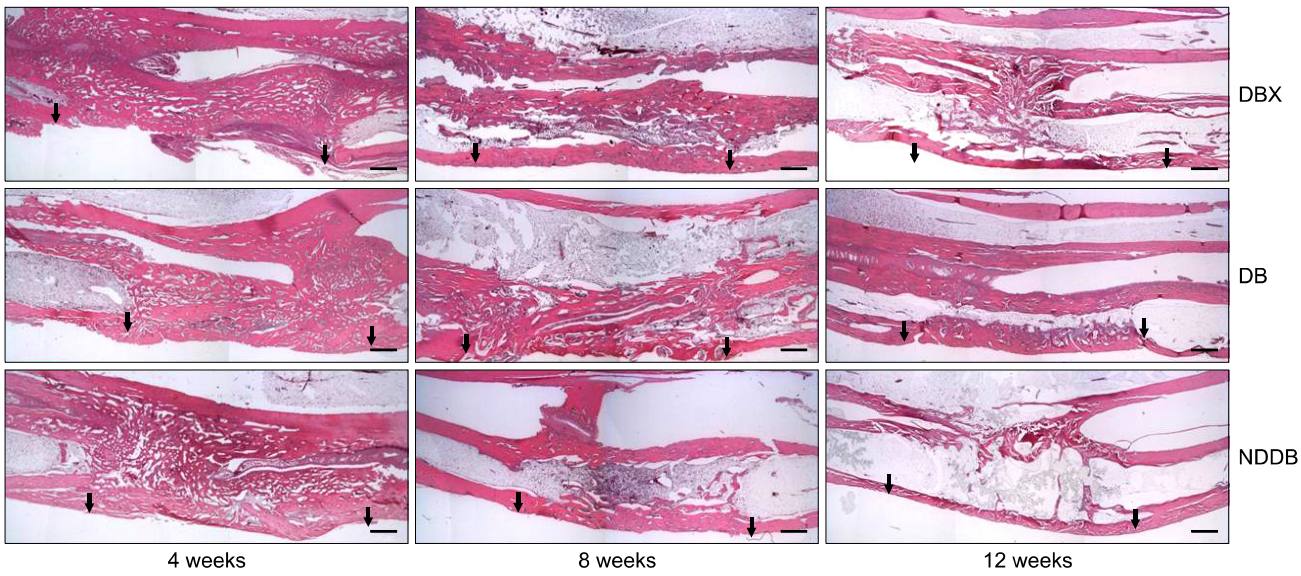

Fig. 6. Light micrograph images taken at 4, 8, and 12 weeks post-implantation. The samples were decalcified and embedded in paraffin. The tissue sections obtained in 4-μm thickness were stained with H&E. The arrow indicates the junction between normal bone and host bone. All experimental groups show considerable new bone formation at the defect sites and the grafted BDMs surrounded by these new bones at 4 weeks post-implantation. All groups show initial signs of marrow formation at 8 weeks. Bone remodeling was nearly complete in all groups at 12 weeks. The magnification was 12.5.

image analysis were 58.93 ± 12.90, 49.25 ± 19.29, and 56.67 ± 17.15 mm^2 in DBX, DB, and DDNB at 4 weeks post-implantation, respectively. These areas decreased further at 8 weeks post-implantation to 22.63 ± 9.77, 23.87 ± 6.55, and 29.97 ± 9.80 mm^2 in DBX, DB and NNDB, respectively. Finally, they were 0.80 ± 0.68, 2.78 ± 1.76, and 3.77 ± 1.30 mm^2 in NBX, DB, and NNDB at 12 weeks post-implantation, respectively. There were no significant differences among groups at 4, 8, and 12 weeks post-implantation (Fig. 7).

Discussion

In the present study, we compared the bone healing effects of three different DBM products (DBX, DB, and NNDB) using various analytical methods such as X-ray, micro-CT and histology in a rabbit radial bone defect model. The results of this study indicated that the three investigated DBM products have comparable bone healing effects with regard to bone healing score, bone mineral density, bone volume fraction, and residual bone area with time, although they have different carrier molecules (HA in DBX *vs.* CMC in DB and NNDB) or bone composition (cortical bone in DBX and DB *vs.* cortical bone with cancellous bone in NNDB). However, this conclusion should be interpreted with caution, because we may miss critical time points between 0 and 4 weeks after implantation, when important osteoconductive and osteoinduction processes are actively ongoing [1]. If we analyzed several points during this period, we would find differences among the three DBM products owing to the use of various analytical methods. This is a limitation of this study that warrants further research. Nevertheless, this is the first report to thoroughly examine comparative bone healing effects of different DBM products using a relatively large bone defect model in rabbits. Previous studies have used a spinal fusion model in athymic nude rats [13,24] or femoral defect model (6 mm diameter and 10 mm deep defect) in rabbits.

DBM has both osteoinductive and osteoconductive activities, whereas cancellous bone has osteoconductive activity [3]. Although different formulations of DBM and cancellous bone can be made, Turner *et al.* [22] reported no difference between them in terms of their bone healing ability in a canine model. In our experiment, DB and NDDB have different ratios of DBM and cancellous bone (only cortical bone in DB *vs.* cortical and cancellous bone in NDDB; 18 : 12), but we also found that there were no differences in bone healing effects between DB and NNDB. When the bone composition was taken into consideration, DBX had lower radiopacity, bone volume fraction and BMD than DB and NDDB, suggesting that it was more effectively demineralized during manufacturing. Indeed, DBX is demineralized with hydrochloric acid so that bone matrix contains less than 8% calcium [18]. Although we did not directly measure the calcium content of DB and NDDB, it should be higher than 8% based on our radiographic and micro-CT data.

It should be noted that different carrier molecules with DBM were used in this study. Specifically, HA is a carrier of DBX, whereas CMC is a carrier for DB and NDDB. Previous studies have already shown that both materials are excellent carriers for bone regeneration. For example, Aslan *et al.* [2] reported that HA played an important role in morphogenesis and tissue healing during bone regeneration. When used as a carrier for bone morphogenetic protein-2, bone formation was enhanced in rat and non-human primate calvarial defect models [11,21]. Reynolds *et al.* [20] proposed that CMC can serve as a thixotrophic agent and function to stabilize polymers and drug delivery vehicles. Cho *et al.* [5] reported that a calcium sulfate-based putty containing CMC promoted early bony consolidation in distraction osteogenesis. When CMC was used to stabilize a collagenous device loaded with osteogenic protein-1, it was also shown that it markedly facilitated regeneration of the mandibular defect [23]. Our finding in this study that there was no difference in bone healing effects between HA-based DBM (DBX) and CMC-based DBM (DB and NNDB) also indicates that there are excellent biocompatibility and biological properties of both carrier molecules.

The seeming discrepancy between an increased radiographic bone healing score and decreased bone volume fraction during the follow-up periods after DBM implantation needs further discussion. During the bone remodeling process, the grafted DBM was resorbed by osteoclasts, while new bone grew from osteoblasts, and thus overall bone mineral density should be constant. The investigation of bone mineral density of the three groups during the experimental periods in our study may support this notion, despite their being slightly decreasing trends that did not differ significantly.

Finally, bone healing efficacy of DBM products is most likely affected by many factors, such as differences in preprocess handling, varying demineralization time, final particle size, terminal sterilization, and differences in carrier molecules [24]. Indeed, the three DBM products investigated in this study had different carriers, ratios of BDM to cancellous bone, and bone parameters upon micro-CT. Although these factors may influence bone healing capacity, our data do not support this argument. In conclusion, the BDM products investigated in this study showed comparable bone healing capacity in a critical-sized radial bone defect model in rabbits.

Acknowledgments

This work was supported by a grant from the Next-Generation BioGreen 21 Program (PJ009744) and

Bio-Industry Technology Development Program (312031-3), MAFRA, Korea. We are grateful to Hans Biomed Corp. for kindly providing us with two bone graft matrices (DB and NNDB).

Conflict of interest

There is no conflict of interest.

References

1. **Albrektsson T, Johansson C.** Osteoinduction, osteoconduction and osseointegration. Eur Spine J 2001, **10** (Suppl 2), S96-101.
2. **Aslan M, Şimşek G, Dayi E.** The effect of hyaluronic acid-supplemented bone graft in bone healing: experimental study in rabbits. J Biomater Appl 2006, **20**, 209-220.
3. **Boyan BD, Ranly DM, McMillan J, Sunwoo M, Roche K, Schwartz Z.** Osteoinductive ability of human allograft formulations. J Periodontol 2006, **77**, 1555-1563.
4. **Chesmel KD, Branger J, Wertheim H, Scarborough N.** Healing response to various forms of human demineralized bone matrix in athymic rat cranial defects. J Oral Maxillofac Surg 1998, **56**, 857-863.
5. **Cho BC, Park JW, Baik BS, Kim IS.** Clinical application of injectable calcium sulfate on early bony consolidation in distraction osteogenesis for the treatment of craniofacial microsomia. J Craniofac Surg 2002, **13**, 465-475.
6. **Cook SD, Barrack RL, Santman M, Patron LP, Salkeld SL, Whitecloud TS 3rd.** Strut allograft healing to the femur with recombinant human osteogenic protein-1. Clin Orthop Relat Res 2000, **381**, 47-57.
7. **Edwards JT, Diegmann MH, Scarborough NL.** Osteoinduction of human demineralized bone: characterization in a rat model. Clin Orthop Relat Res 1998, **357**, 219-228.
8. **Han B, Tang B, Nimni ME.** Combined effects of phosphatidylcholine and demineralized bone matrix on bone induction. Connect Tissue Res 2003, **44**, 160-166.
9. **Hopp SG, Dahners LE, Gilbert JA.** A study of the mechanical strength of long bone defects treated with various bone autograft substitutes: an experimental investigation in the rabbit. J Orthop Res 1989, **7**, 579-584.
10. **Jang CH, Park H, Cho YB, Song CH.** Mastoid obliteration using a hyaluronic acid gel to deliver a mesenchymal stem cells-loaded demineralized bone matrix: an experimental study. Int J Pediatr Otorhinolaryngol 2008, **72**, 1627-1632.
11. **Kim J, Kim IS, Cho TH, Lee KB, Hwang SJ, Tae G, Noh I, Lee SH, Park Y, Sun K.** Bone regeneration using hyaluronic acid-based hydrogel with bone morphogenic protein-2 and human mesenchymal stem cells. Biomaterials 2007, **28**, 1830-1837.
12. **Lasa C Jr, Hollinger J, Drohan W, MacPhee M.** Delivery of demineralized bone powder by fibrin sealant. Plast Reconstr Surg 1995, **96**, 1409-1417.
13. **Lee YP, Jo M, Luna M, Chien B, Lieberman JR, Wang JC.** The efficacy of different commercially available demineralized bone matrix substances in an athymic rat model. J Spinal Disord Tech 2005, **18**, 439-444.
14. **Leupold JA, Barfield WR, An YH, Hartsock LA.** A comparison of ProOsteon, DBX, and collagraft in a rabbit model. J Biomed Mater Res B Appl Biomater 2006, **79B**, 292-297.
15. **Matzenbacher SA, Mailhot JM, McPherson JC 3rd, Cuenin MF, Hokett SD, Sharawy M, Peacock ME.** In vivo effectiveness of a glycerol-compounded demineralized freeze-dried bone xenograft in the rat calvarium. J Periodontol 2003, **74**, 1641-1646.
16. **Morone MA, Boden SD.** Experimental posterolateral lumbar spinal fusion with a demineralized bone matrix gel. Spine 1998, **23**, 159-167.
17. **Oakes DA, Lee CC, Lieberman JR.** An evaluation of human demineralized bone matrices in a rat femoral defect model. Clin Orthop Relat Res 2003, **413**, 281-290.
18. **Peterson B, Whang PG, Iglesias R, Wang JC, Lieberman JR.** Osteoinductivity of commercially available demineralized bone matrix: preparations in a spine fusion model. J Bone Joint Surg Am 2004, **86**, 2243-2250.
19. **Pinholt EM, Solheim E, Bang G, Sudmann E.** Bone induction by composite of bioerodible polyorthoester and demineralized bone matrix in rats. Acta Orthop Scand 1991, **62**, 476-480.
20. **Reynolds MA, Aichelmann-Reidy ME, Kassolis JD, Prasad HS, Rohrer MD.** Calcium sulfate-carboxymethylcellulose bone graft binder: histologic and morphometric evaluation in a critical size defect. J Biomed Mater Res B Appl Biomater 2007, **83B**, 451-458.
21. **Takahashi Y, Yamamoto M, Yamada K, Kawakami O, Tabata Y.** Skull bone regeneration in nonhuman primates by controlled release of bone morphogenetic protein-2 from a biodegradable hydrogel. Tissue Eng 2007, **13**, 293-300.
22. **Turner TM, Urban RM, Hall DJ, Infanger S, Gitelis S, Petersen DW, Haggard WO.** Osseous healing using injectable calcium sulfate-based putty for the delivery of demineralized bone matrix and cancellous bone chips. Orthopedics 2003, **26** (Suppl 5), s571-575.
23. **Wang H, Springer ING, Schildberg H, Acil Y, Ludwig K, Rueger DR, Terheyden H.** Carboxymethylcellulose-stabilized collagenous rhOP-1 device-a novel carrier biomaterial for the repair of mandibular continuity defects. J Biomed Mater Res A 2004, **68A**, 219-226.
24. **Wang JC, Alanay A, Mark D, Kanim LEA, Campbell PA, Dawson EG, Lieberman JR.** A comparison of commercially available demineralized bone matrix for spinal fusion. Eur Spine J 2007, **16**, 1233-1240.
25. **Younger EM, Chapman MW.** Morbidity at bone graft donor sites. J Orthop Trauma 1989, **3**, 192-195.